



**AFRL-RQ-WP-TP-2013-0224**

**A DYNAMIC MODELING TOOLBOX FOR AIR VEHICLE  
VAPOR CYCLE SYSTEMS (POSTPRINT)**

**Megan Kania, Justin Koeln, and Andrew Alleyne**

**University of Illinois**

**Kevin McCarthy and Ning Wu**

**P.C. Krause and Associates**

**Soumya Patnaik**

**Mechanical and Thermal Systems Branch**

**Power and Control Division**

**OCTOBER 2013**

**Approved for public release; distribution unlimited.**

*See additional restrictions described on inside pages*

**STINFO COPY**

**© 2012 SAE International**

**AIR FORCE RESEARCH LABORATORY  
AEROSPACE SYSTEMS DIRECTORATE  
WRIGHT-PATTERSON AIR FORCE BASE, OH 45433-7542  
AIR FORCE MATERIEL COMMAND  
UNITED STATES AIR FORCE**

## NOTICE AND SIGNATURE PAGE

Using Government drawings, specifications, or other data included in this document for any purpose other than Government procurement does not in any way obligate the U.S. Government. The fact that the Government formulated or supplied the drawings, specifications, or other data does not license the holder or any other person or corporation; or convey any rights or permission to manufacture, use, or sell any patented invention that may relate to them.

This report was cleared for public release by the USAF 88th Air Base Wing (88 ABW) Public Affairs Office (PAO) and is available to the general public, including foreign nationals.

Copies may be obtained from the Defense Technical Information Center (DTIC)  
(<http://www.dtic.mil>).

AFRL-RQ-WP-TR-2013-0224 HAS BEEN REVIEWED AND IS APPROVED FOR PUBLICATION IN ACCORDANCE WITH ASSIGNED DISTRIBUTION STATEMENT.

\*//Signature//

---

SOUMYA PATNAIK  
Program Manager  
Mechanical and Thermal Systems Branch  
Power and Control Division

//Signature//

---

THOMAS L. REITZ, Technical Advisor  
Mechanical and Thermal Systems Branch  
Power and Control Division  
Aerospace Systems Directorate

//Signature//

---

JOHN G. NAIRUS, Chief Engineer  
Power and Control Division  
Aerospace Systems Directorate

This report is published in the interest of scientific and technical information exchange, and its publication does not constitute the Government's approval or disapproval of its ideas or findings.

\*Disseminated copies will show “//Signature//” stamped or typed above the signature blocks.

# REPORT DOCUMENTATION PAGE

*Form Approved*  
OMB No. 0704-0188

The public reporting burden for this collection of information is estimated to average 1 hour per response, including the time for reviewing instructions, searching existing data sources, gathering and maintaining the data needed, and completing and reviewing the collection of information. Send comments regarding this burden estimate or any other aspect of this collection of information, including suggestions for reducing this burden, to Department of Defense, Washington Headquarters Services, Directorate for Information Operations and Reports (0704-0188), 1215 Jefferson Davis Highway, Suite 1204, Arlington, VA 22202-4302. Respondents should be aware that notwithstanding any other provision of law, no person shall be subject to any penalty for failing to comply with a collection of information if it does not display a currently valid OMB control number. **PLEASE DO NOT RETURN YOUR FORM TO THE ABOVE ADDRESS.**

<b>1. REPORT DATE (DD-MM-YY)</b> October 2013		<b>2. REPORT TYPE</b> Conference Proceedings Postprint		<b>3. DATES COVERED (From - To)</b> 08 February 2012 – 01 October 2012	
<b>4. TITLE AND SUBTITLE</b> A DYNAMIC MODELING TOOLBOX FOR AIR VEHICLE VAPOR CYCLE SYSTEMS (POSTPRINT)				<b>5a. CONTRACT NUMBER</b> FA8650-12-C-2231	
				<b>5b. GRANT NUMBER</b>	
				<b>5c. PROGRAM ELEMENT NUMBER</b> 65502F	
<b>6. AUTHOR(S)</b> Megan Kania, Justin Koeln, and Andrew Alleyne (University of Illinois) Kevin McCarthy and Ning Wu (P.C. Krause and Associates) Soumya Patnaik (AFRL/RQQM)				<b>5d. PROJECT NUMBER</b> 3005	
				<b>5e. TASK NUMBER</b>	
				<b>5f. WORK UNIT NUMBER</b> Q0V2	
<b>7. PERFORMING ORGANIZATION NAME(S) AND ADDRESS(ES)</b> University of Illinois 158 MEB 1206 W. Green Street Urbana, IL 61801 ----- P.C. Krause and Associates 3000 Kent Avenue, Suite C1-100 West Lafayette, IN 47906				<b>8. PERFORMING ORGANIZATION REPORT NUMBER</b>	
Mechanical and Thermal Systems Branch (AFRL/RQQM) Power and Control Division Air Force Research Laboratory Aerospace Systems Directorate Wright-Patterson Air Force Base, OH 45433-7542 Air Force Materiel Command, United States Air Force					
<b>9. SPONSORING/MONITORING AGENCY NAME(S) AND ADDRESS(ES)</b> Air Force Research Laboratory Aerospace Systems Directorate Wright-Patterson Air Force Base, OH 45433-7542 Air Force Materiel Command United States Air Force				<b>10. SPONSORING/MONITORING AGENCY ACRONYM(S)</b> AFRL/RQQM	
				<b>11. SPONSORING/MONITORING AGENCY REPORT NUMBER(S)</b> AFRL-RQ-WP-TP-2013-0224	
<b>12. DISTRIBUTION/AVAILABILITY STATEMENT</b> Approved for public release; distribution unlimited.					
<b>13. SUPPLEMENTARY NOTES</b> PA Case Number: 88ABW-2012-3165; Clearance Date: 04 Jun 2012. This paper contains color.  This conference paper is published in the Proceedings of 2012 SAE Power Systems Conference, a conference that was held in Phoenix, Arizona, October 30 through November 1, 2012. © 2012 SAE International. The U.S. Government is joint author of the work and has the right to use, modify, reproduce, release, perform, display, or disclose the work.					
<b>14. ABSTRACT</b> Modern air vehicles face increasing internal heat loads that must be appropriately understood in design and managed in operation. This paper examines one solution to creating more efficient and effective thermal management systems (TMSs): vapor cycle systems (VCSs). VCSs are increasingly being investigated by aerospace government and industry as a means to provide much greater efficiency in moving thermal energy from one physical location to another. In this work, we develop the Air Force Research Laboratory Transient Thermal Modeling and Optimization (ATTMO) toolbox: a modeling and simulation tool based in Matlab/Simulink that is suitable for understanding, predicting, and designing a VCS. The ATTMO toolbox also provides capability for understanding the VCS as part of a larger air vehicle system. The toolbox is presented in a modular fashion whereby the individual components are presented along with the framework for interconnecting them. The modularity allows for easy user re-configurability as well as the ability to scale from simple to full vehicle systems. A computational environment is discussed that allows for simulations running many times faster than real time. Simulation results are presented for a laboratory scale test stand system consisting of both single and multiple evaporators. The simulations are verified against experimental results demonstrating the potential of the tool.					
<b>15. SUBJECT TERMS</b> VCS, vapor cycle system, VCS modeling, ATTMO, AFRL Transient Thermal Modeling and Optimization					
<b>16. SECURITY CLASSIFICATION OF:</b>			<b>17. LIMITATION OF ABSTRACT:</b> SAR	<b>18. NUMBER OF PAGES</b> 20	<b>19a. NAME OF RESPONSIBLE PERSON (Monitor)</b> Soumya Patnaik <b>19b. TELEPHONE NUMBER (Include Area Code)</b> N/A
<b>a. REPORT</b> Unclassified	<b>b. ABSTRACT</b> Unclassified	<b>c. THIS PAGE</b> Unclassified			

## A Dynamic Modeling Toolbox for Air Vehicle Vapor Cycle Systems

2012-01-2172

Published  
10/22/2012

Megan Kania, Justin Koeln and Andrew Alleyne  
University of Illinois

Kevin McCarthy and Ning Wu  
P.C. Krause and Associates Inc

Soumya Patnaik  
US Air Force Research Laboratory

Copyright © 2012 SAE International  
doi:10.4271/2012-01-2172

### **ABSTRACT**

Modern air vehicles face increasing internal heat loads that must be appropriately understood in design and managed in operation. This paper examines one solution to creating more efficient and effective thermal management systems (TMSs): vapor cycle systems (VCSs). VCSs are increasingly being investigated by aerospace government and industry as a means to provide much greater efficiency in moving thermal energy from one physical location to another. In this work, we develop the AFRL (Air Force Research Laboratory) Transient Thermal Modeling and Optimization (ATTMO) toolbox: a modeling and simulation tool based in Matlab/Simulink that is suitable for understanding, predicting, and designing a VCS. The ATTMO toolbox also provides capability for understanding the VCS as part of a larger air vehicle system. The toolbox is presented in a modular fashion whereby the individual components are presented along with the framework for interconnecting them. The modularity allows for easy user re-configurability as well as the ability to scale from simple to full vehicle systems. A computational environment is discussed that allows for simulations running many times faster than real-time. Simulation results are presented for a laboratory scale test stand system consisting of both single and multiple evaporators. The simulations are verified against experimental results demonstrating the potential of the tool.

### **1. INTRODUCTION**

With the progression toward more electronic aircraft in combination with low thermal conductivity composite skins and reduced ram heat exchanger inlets, thermal loads from a range of subsystems must be understood and managed via thermal management systems (TMSs). Due to their efficiency, vapor cycle systems (VCSs) are used to meet a wide variety of thermal management needs including residential, automotive, and commercial air-conditioning and refrigeration. These systems come in a wide range of sizes and architectures to handle various thermal loads.

The focus of this paper is to present the development and capabilities of the AFRL (Air Force Research Laboratory) Transient Thermal Modeling and Optimization (ATTMO) toolbox based in the Matlab/Simulink environment. A similar toolbox, named TMS toolbox, has previously been developed to simulate and optimize TMS performance [1]. The ATTMO toolbox is able to interface with the TMS toolbox, providing the ability to simulate VCSs as part of the larger TMS. The modularity of this tool allows for a variety of VCS configurations, including single and dual evaporator architectures, and can be incorporated with vehicle, propulsion, and power subsystem models to provide a complete understanding of the interactions between subsystems. Using a first-principles based approach, the ATTMO toolbox allows the user to better understand, predict, and control the behavior of VCSs, from design through implementation. Through better understanding of system dynamics, this tool can aid in the design and control of VCSs

to better meet the growing thermal management needs of these aircraft.

The paper is organized as follows. First, an overview of a VCS is given in Section 2, with a focus on the cycle and operation description. Then, the basic components of the cycle and their governing equations are presented in Section 3. Construction of a dual evaporator model in the toolbox framework is presented in Section 4. Section 5 gives an introduction to the physical test stand at the University of Illinois at Urbana-Champaign. In Section 6, data is presented to show the agreement between the model and a physical test stand thereby verifying the modeling and simulation approach taken. Finally, we present our conclusions and future work in Sections 7 and 8.

## 2. VCS OVERVIEW

A standard VCS consists of four major components: compressor, condenser, valve, and evaporator [2]. The standard cycle has four states, depicted in Figure 1 as (1,2,3,4), and two pressures,  $P_{cond}$  and  $P_{evap}$ . The transition from state  $i$  to state  $j$  is indicated by  $i - j$ . Four simplifying assumptions are typically used: isentropic compression (1 - 2), isobaric condensation (2 - 3), isenthalpic expansion (3 - 4), and isobaric evaporation (4 - 1). Low pressure superheated vapor enters the compressor and exits at a high pressure and temperature. The condenser transfers the heat from the refrigerant to the cooler secondary fluid and the refrigerant exits as either a subcooled liquid or a two-phase mixture. The refrigerant is expanded through the valve, exiting as a lower pressure, two-phase mixture. The evaporator transfers heat from the warmer secondary fluid to the refrigerant, which exits as a low pressure, superheated vapor. This superheated vapor then enters the compressor and the cycle repeats.

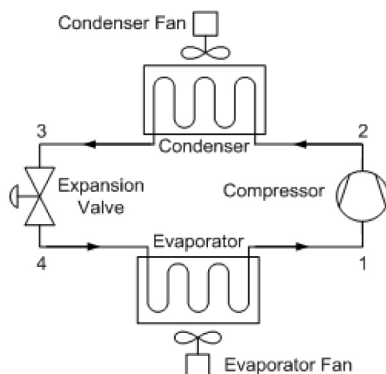


Figure 1. Schematic of a vapor cycle system (VCS)

A VCS has a variety of user-actuated controls which provide the ability to control the thermodynamic state of the refrigerant at each of the four locations seen in Figure 1. These control inputs include the total mass of refrigerant in the cycle, known as the charge of the system, the compressor

speed, valve opening, and secondary fluid mass flow rates for the heat exchangers, all of which affect the dynamics and efficiency of the cycle. Additionally, the phase of the refrigerant in the condenser and evaporator (i.e. subcooled liquid, two-phase mixture, or superheated vapor) affects the quantity of energy transferred in the cycle. Modeling of VCSs provides the required insight to the highly nonlinear and coupled relationships between these control inputs and the system dynamics necessary to develop more advanced and higher performance control strategies.

## 3. COMPONENT MODELING

The Thermosys modeling platform, developed at the University of Illinois at Urbana-Champaign, serves as the foundation of the ATTMO toolbox. The fundamental equations of the VCS components presented below, are also used in the Thermosys framework. Thermosys has been validated both at steady-state and under transient conditions with a number of experimental VCSs, including the test stand in Section 5 [3,4,5,6]. Due to the accuracy of the Thermosys models during transient system behavior, this framework has been used for the development and implementation of various control strategies, which require more than an understanding of steady-state behavior.

The ATTMO toolbox was developed in the Matlab/Simulink environment. Simulink offers a variety of numerical integration solvers including fixed step solvers of various order and variable step, stiff solvers. The fixed step solvers can be used for hardware-in-the-loop applications where real-time model simulation is required [7]. The stiff solvers can be used when a system has multiple, different time scale dynamics, such as the quick pressure dynamic and the slow thermal dynamic in a VCS. The graphical nature of the Simulink environment is similar to a system schematic, making model development and navigation simple and intuitive. This environment also allows for simple integration of control strategies within the modeling framework, such as embedded system emulation [7].

The components in the ATTMO toolbox can be divided into four basic categories: system actuation devices, heat exchangers, flow passageways, and support functions, as shown in Figure 2. The modularity of the toolbox allows the user to simply drag and drop components into the Simulink model and connect individual components with a buss structure which contains information about the state of the refrigerant. Each component has a mask which allows the user to specify parameters and operation conditions specific to the component.

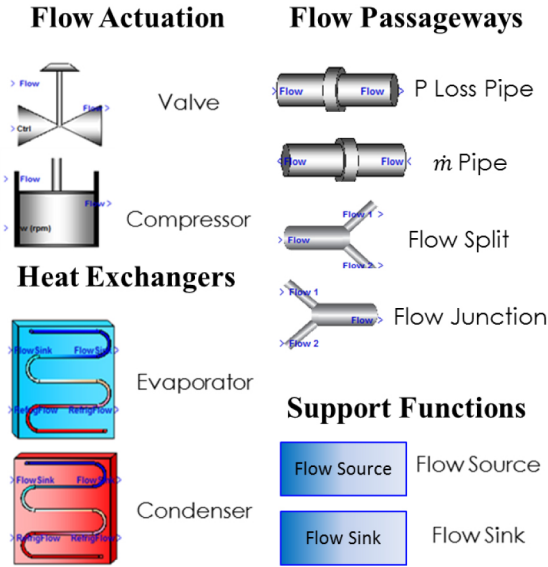


Figure 2. Components available in the ATTMO toolbox

Figure 3 shows how the basic VCS discussed in Section 2 would be modeled using this toolbox. The figure also shows how the busses are used to connect individual components. The busses contain the information required to completely define the state of the refrigerant: pressure, enthalpy, and mass flow rate, as well as temperature for easy comparison to measured system data. Refrigerant property information was taken from the Engineering Equation Solver (EES), a program generally used in HVAC research. The modeling framework used in this toolbox requires the alternation of pressure calculating devices, e.g. the heat exchangers, and mass flow rate calculating devices, e.g. the compressor. This is reflected in Figure 3 where pressure calculating components are highlighted in red and mass flow calculating components are highlighted in green. While this is intuitive for a simple system, more complex systems may require additional components to achieve this alternation and will be discussed in greater detail in Section 4. The system shown in Figure 3 also uses two of the support blocks: the Flow Source and the Flow Sink. These components allow the user to directly specify the state of a fluid. In the current system they are used to specify the properties of the secondary fluid (air for the systems verified in Section 6) for each of the heat exchangers, but can also be used to begin or terminate refrigerant flow.

Typically, a single component may require information from upstream and downstream components. For example, the condenser requires both the mass flow rate determined by the compressor and the mass flow rate determined by the valve in order to calculate the refrigerant pressure. Each component in the ATTMO toolbox is capable of forming these upstream and downstream paths of information transfer automatically when the user connects components using the buss structure. A single buss structure to connect component blocks

significantly reduces model development time over a series of single connections for each variable of interest.

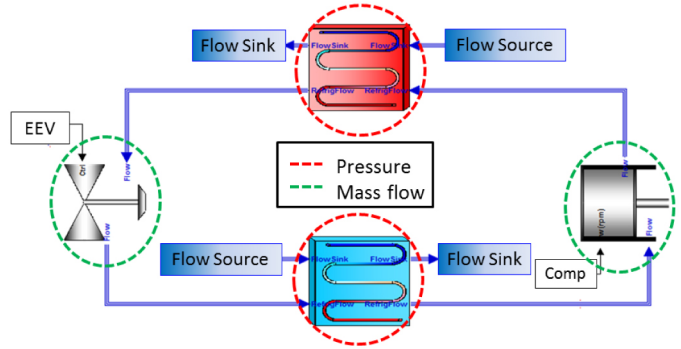


Figure 3. Single evaporator model with the pressure and mass flow calculating components highlighted

### 3.1. Valves

Valves are used to bring high pressure refrigerant from the exit of the condenser down to a low pressure for the evaporator. Four different types of valves are modeled in the toolbox: automatic expansion valve (AEV), electronic expansion valve (EEV), orifice tube (OT), and thermostatic expansion valve (TEV). Each valve model calculates the refrigerant mass flow through the valve based on the inlet and outlet pressures and a control input.

Control signals are sent to the AEV, EEV, and TEV to determine valve opening area. The orifice tube is a static component and does not have a control signal. The EEV opening is directly defined by the user or by a user developed controller. The AEV attempts to maintain a constant pressure in either the condenser or evaporator, depending on how the AEV is interfaced. The TEV works with the evaporator to maintain a constant refrigerant superheat at the exit of the evaporator.

All four of the valves use Equation (1) to calculate refrigerant mass flow rate. As shown in Figure 3, components which calculate pressure alternate with components that calculate mass. Pressure is a state variable within the heat exchangers, so the mass calculation must be done by the remaining two components: the valve and compressor. The discharge coefficient,  $C_d$ , is experimentally determined over the range of operating conditions and is implemented via a lookup table based on the parameters of interest. Figure 4 shows a sample mapping for an EEV where  $C_d$  is a function of valve opening and the pressure drop across the valve [8]. The AEV uses the regulated heat exchanger pressure and the pressure difference across the valve to determine  $C_d$ . The TEV uses two maps,  $C_d$  a map which is based on the pressure differential and the force exerted on the TEV, and an area map which is based on the pressure difference between the TEV sensing bulb and the evaporator pressure. The user defined constant,  $K_v$ , can be

used to adjust for small deviations between experimental and simulated refrigerant mass flow rates caused by the un-modeled factors such as friction.  $K_v$  may be set to 1 if the deviations between experimental and simulated data are unknown.

$$\dot{m} = K_v C_d A_v \sqrt{\rho(\Delta P)} \quad (1)$$

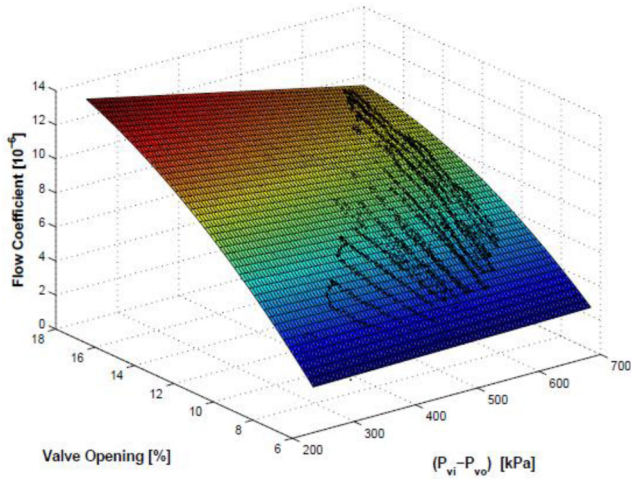


**Figure 4. Sample flow coefficient map for the EEV, with black points representing experimental data**

## 3.2. Compressor

The compressor, in combination with the valve, sets the mass flow rate in the VCS and raises the refrigerant from a low pressure vapor at the outlet of the evaporator to a high pressure and high temperature vapor which enters the condenser. A standard VCS modeling assumption is that the compressor operates isentropically. In this work, the compressor model uses an adiabatic efficiency correction

factor map,  $\eta_h = f\left(\omega, \frac{P_{out}}{P_{in}}\right)$ , for the outlet enthalpy calculation and a volumetric efficiency correction factor map,

$\eta_m = f\left(\omega, \frac{P_{out}}{P_{in}}\right)$ , for the refrigerant mass flow rate to improve the accuracy of the model. Both  $P_{cond}$  and  $P_{evap}$  are

used to define the pressure ratio,  $\frac{P_{out}}{P_{in}}$ . These correction factors need to be determined experimentally for a particular compressor. While the VCS is in operation, the same compression process which raised the pressure and temperature of the refrigerant also heats the metal shell of the compressor, which has a significant thermal capacitance. This heat transfer can be approximated as first order dynamic with a time constant,  $\tau_{shell}$ , which depends on the mass of the compressor. Since the mass flow dynamics of the VCS are significantly faster than the thermal dynamics, the compressor can often be treated as a quasi-static component,

with the refrigerant mass flow rate determined statically, but the enthalpy determined dynamically.

Equations (2), (3), (4) outline the behavior of the compressor model utilized in this toolbox. As with the valve,  $K_m$  and  $K_h$  are user defined values, which account for differences in mass flow rate caused by un-modeled factors which may not have been captured in the maps. The  $h_{static}$  variable in Equation (3) refers to the refrigerant enthalpy if there was no heat transfer from the compressor shell. The enthalpy of the refrigerant leaving the compressor has a first order dynamic, shown in Equation (4), which captures the thermal capacitance of the compressor.

$$\dot{m} = \omega V \rho \eta_m K_m \quad (2)$$

$$h_{static} = h_{in} + \frac{h_{out,S} - h_{in}}{\eta_h K_h} \quad (3)$$

$$\dot{h}_{out} = \frac{h_{static} - h_{out}}{\tau_{shell}} \quad (4)$$

## 3.3. Evaporator

When a VCS is used to provide cooling, the evaporator transfers heat from the cooled space or medium (known as the secondary fluid) to the refrigerant causing the refrigerant density to decrease, ideally creating a superheated vapor at the evaporator outlet to prevent damage to the compressor. Currently, the heat exchangers in the ATTMO toolbox are limited to interfacing with air as the secondary fluid and the development of a liquid-to-liquid heat exchanger is left for future work. Refrigerant traveling through a heat exchanger is assumed to be at a single pressure determined by the model.

The evaporator uses a lumped parameter modeling assumption for the generation of its governing equations [9,10,11,12,13,14]. As shown in Figure 5, the evaporator contains two-phase fluid and superheated vapor or just two-phase fluid, depending on the conditions of the heat transfer [4]. Within each region, the heat transfer correlations between the refrigerant, pipe walls, and secondary fluid are assumed to be constant. Therefore, it is possible to treat the evaporator as a two zone model, with a moving boundary interface between the two-phase and the superheated vapor lengths. In operation, the user may have access to state information at the inlet and outlet of the evaporator. While some of these states can be measured experimentally, such as pressure and temperature, other states, such as the length of the two-phase region, would be very difficult to measure in most applications. The VSC model is able to provide this information, which could be useful in developing advanced control strategies.

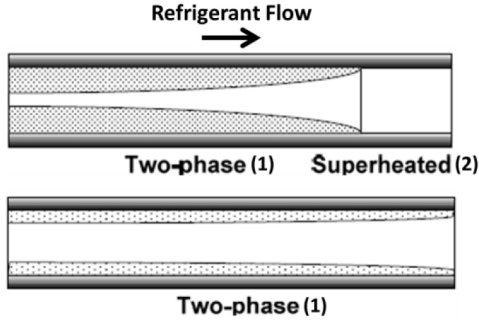


Figure 5. Refrigerant modes within the evaporator

Equations (5), (6), (7), (8), (9) determine the states of the evaporator,  $[\zeta_1 P h_2 \gamma m_{12}]^T$ , whose derivatives are calculated from the equations below. Equations (5) and (6) are the conservation of mass and conservation of energy equations for the superheat zone, respectively. Equations (7) and (8) are the conservation of mass and energy in the two-phase zone, respectively. Equation (9) is the void fraction calculation for the two-phase zone. The void fraction,  $\gamma$ , refers to the volume of gas versus liquid in the two-phase mixture for a localized region of fluid. Here, the  $\bar{\gamma}$  represents the mean void fraction in a region and  $\bar{\gamma}_{tot}$  is the equilibrium mean void fraction for complete condensation, defined for both the condenser and evaporator, from saturated vapor to saturated liquid. The subscripts represent the zone of the refrigerant, with 1 referring to the two-phase zone and 2 referring to the superheat zone, the inlet and outlet conditions, or the vapor and liquid transitions of the refrigerant. Also, all of the  $h$  values used in the equations refer to the refrigerant enthalpy, not the heat transfer coefficient.

$$\frac{d\zeta_1}{dt} - \frac{\zeta_2}{\rho_2} \frac{\partial \rho_2}{\partial P} \frac{dP}{dt} - \frac{\zeta_2}{\rho_2} \frac{\partial \rho_2}{\partial h_2} \frac{dh_2}{dt} + \frac{\dot{m}_{12}}{\rho_2 V} = \frac{\dot{m}_{out}}{\rho_2 V} \quad (5)$$

$$-\frac{1}{\rho_2} \frac{dP}{dt} + \frac{dh_2}{dt} - \frac{h_g - h_2}{\rho_2 V \zeta_2} \dot{m}_{12} = \frac{\dot{Q}_2 - \dot{m}_{out}(h_2 - h_g)}{\rho_2 V \zeta_2} \quad (6)$$

$$\frac{d\zeta_1}{dt} + \frac{\zeta_1}{\rho_1} \frac{\partial \rho_1}{\partial P} \frac{dP}{dt} + \frac{\zeta_1}{\rho_1} \frac{\partial \rho_1}{\partial \bar{\gamma}} \frac{d\bar{\gamma}}{dt} + \frac{\dot{m}_{12}}{\rho_1 V} = \frac{\dot{m}_{in}}{\rho_1 V} \quad (7)$$

$$\left[ \frac{\partial h_1}{\partial P} - \frac{1}{\rho_1} \right] \frac{dP}{dt} + \frac{\partial h_1}{\partial \bar{\gamma}} \frac{d\bar{\gamma}}{dt} + \frac{h_g - h_1}{\rho_1 V \zeta_1} \dot{m}_{12} = \frac{\dot{Q}_1 + \dot{m}_{in}(h_{in} - h_1)}{\rho_1 V \zeta_1} \quad (8)$$

$$\frac{\partial \bar{\gamma}_{tot}}{\partial P} \frac{dP}{dt} - \frac{d\bar{\gamma}}{dt} = K_\gamma (\bar{\gamma} - \bar{\gamma}_{tot}) \quad (9)$$

Additionally, the evaporator calculates the time derivative of the wall temperatures in both regions, shown in Equations (10) and (11). allows the wall temperatures to vary as the length of each zone varies within the evaporator. If the length of the two-phase region is increasing, and if the length of the superheat region is increasing,  $T_{r1} = T_{wall1}$ . The wall

temperatures play a critical role in modeling the heat transfer from the secondary fluid to the refrigerant in the evaporator.

$$\dot{T}_{wall1} = \frac{1}{\zeta_1} \left[ (T_{r1} - T_{wall1}) \dot{\zeta}_1 - \frac{\dot{Q}_{ref1} + \dot{Q}_{sec1}}{c_{pwall} m_{wall}} \right] \quad (10)$$

$$\dot{T}_{wall2} = \frac{1}{\zeta_2} \left[ (T_{wall2} - T_{r1}) \dot{\zeta}_1 - \frac{\dot{Q}_{ref2} + \dot{Q}_{sec2}}{c_{pwall} m_{wall}} \right] \quad (11)$$

Additional information on the derivation of these equations as well as details on the conditions for the disappearance and reappearance of the superheated zone under transient system dynamics can be found in [4].

### 3.4. Condenser

Converse to the evaporator, the condenser transfers heat from the refrigerant to the secondary fluid, causing the refrigerant enthalpy to decrease and the refrigerant density to increase. The refrigerant at the condenser outlet is ideally subcooled liquid. A subcooled liquid would insure all of the heat transfer possible in the two-phase region has occurred, resulting in high efficiency. However, too much subcooling is an indication that the condenser is oversized for the system. The condenser model assumes isobaric refrigerant. The condenser calculates pressure, and uses air as the secondary fluid for the validation in Section 6.

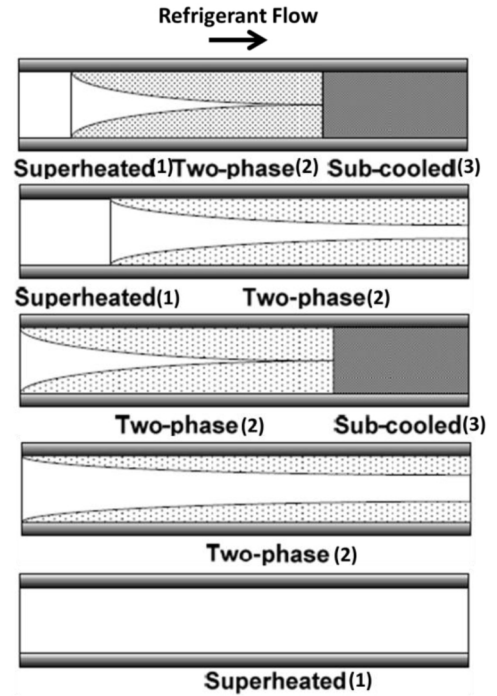


Figure 6. Refrigerant modes within the condenser

Similar to the evaporator, the condenser uses a lumped parameter modeling assumption for the generation of its governing equations. As shown in Figure 6, the condenser can contain superheated vapor, a two-phase mixture, and

subcooled liquid. Therefore, there are five modes of operation in the condenser, corresponding to the combinations of these three zones [4]. The condenser can be treated as a three zone moving boundary model, with boundaries defined by the superheat - two-phase interface and the two-phase - subcooled interface.

Equations (12), (13), (14), (15), (16), (17), (18), (19) determine the state of the condenser,  $[\zeta_1 \zeta_2 P h_3 m_{12} m_{23} h_1 \gamma]^T$ , whose derivatives are calculated from the equations below. Equations (12) and (13) are the conservation of mass and conservation of energy equations for the subcooled zone, respectively. Equations (14) and (15) are the conservation of mass and conservation of energy equations for the superheat zone, respectively. Equation (16) calculates an enthalpy average in the superheat zone. Equations (17) and (18) are the conservation of mass and conservation of energy equations for the two-phase zone, respectively. Equation (19) determines the void fraction of the two-phase zone. Unlike the evaporator equations, the superheat zone is 1, the two-phase zone is 2, and the subcooled zone is 3.

$$\frac{d\zeta_1}{dt} + \frac{d\zeta_2}{dt} - \frac{\zeta_3}{\rho_3} \frac{dh_3}{dt} + \frac{\dot{m}_{23}}{\rho_3 V} = \frac{\dot{m}_{out}}{\rho_3 V} \quad (12)$$

$$\frac{dh_3}{dt} - \frac{h_f - h_3}{\rho_3 V \zeta_3} \dot{m}_{23} - \frac{1}{\rho_3} \frac{dP}{dt} = \frac{\dot{Q}_3}{\rho_3 V \zeta_3} \quad (13)$$

$$\frac{d\zeta_1}{dt} + \frac{\zeta_1}{\rho_1} \frac{\partial \rho_1}{\partial P} \frac{dP}{dt} + \frac{\dot{m}_{12}}{\rho_1 V} = \frac{\dot{m}_{in}}{\rho_1 V} \quad (14)$$

$$\frac{dh_1}{dt} - \frac{1}{\rho_1} \frac{dP}{dt} + \frac{h_g - h_1}{\rho_1 V \zeta_1} \dot{m}_{12} = \frac{\dot{Q}_1 + \dot{m}_{in}(h_{in} - h_1)}{\rho_1 V \zeta_1} \quad (15)$$

$$\frac{dh_1}{dt} = \frac{1}{2} \left( \frac{dh_{in}}{dt} + \frac{dh_g}{dt} \right) = \frac{1}{2} \frac{dh_{in}}{dt} + \frac{1}{2} \frac{\partial h_g}{\partial P} \frac{dP}{dt} \quad (16)$$

$$\frac{d\zeta_2}{dt} + \frac{\zeta_2}{\rho_2} \frac{\partial \rho_2}{\partial P} \frac{dP}{dt} + \frac{\dot{m}_{23}}{\rho_2 V} - \frac{\dot{m}_{12}}{\rho_2 V} + \frac{\zeta_2}{\rho_2} \frac{\partial \rho_2}{\partial \bar{\gamma}} \frac{d\bar{\gamma}}{dt} = 0 \quad (17)$$

$$\left[ \frac{\partial h_2}{\partial P} - \frac{1}{\rho_2} \right] \frac{dP}{dt} + \frac{h_f - h_2}{\rho_2 V \zeta_2} \dot{m}_{23} - \frac{h_g - h_2}{\rho_2 V \zeta_2} \dot{m}_{12} + \frac{\partial h_2}{\partial \bar{\gamma}} \frac{d\bar{\gamma}}{dt} = \frac{\dot{Q}_2}{\rho_2 V \zeta_2} \quad (18)$$

$$\frac{\partial \bar{\gamma}_{tot}}{\partial P} \frac{dP}{dt} - \frac{d\bar{\gamma}}{dt} = K_\gamma (\bar{\gamma} - \bar{\gamma}_{tot}) \quad (19)$$

Additionally, the condenser calculates the time derivative of the wall temperatures in all three regions, shown in Equations (20), (21), (22).  $T_{r1}$  refers to the interaction area between the two-phase and superheat zones and  $T_{r2}$  refers to the two-phase and subcooled zones. As with the evaporator,  $T_r$  takes on the temperature of the zone which is decreasing in length.

$$\dot{T}_{wall1} = \frac{1}{\zeta_1} \left[ (T_{r1} - T_{wall1}) \dot{\zeta}_1 - \frac{\dot{Q}_{ref1} + \dot{Q}_{sec1}}{c_{pwall} m_{wall}} \right] \quad (20)$$

$$\dot{T}_{wall2} = \frac{1}{\zeta_2} \left[ (\dot{\zeta}_1 + \dot{\zeta}_2) T_{r2} - \dot{\zeta}_1 T_{r1} - \dot{\zeta}_2 T_{wall2} - \frac{\dot{Q}_{ref2} + \dot{Q}_{sec2}}{c_{pwall} m_{wall}} \right] \quad (21)$$

$$\dot{T}_{wall3} = \frac{1}{\zeta_3} \left[ (\dot{\zeta}_1 + \dot{\zeta}_2) (T_{wall3} - T_{r2}) - \frac{\dot{Q}_{ref3} + \dot{Q}_{sec3}}{c_{pwall} m_{wall}} \right] \quad (22)$$

Once again, additional information on the modeling of the condenser can be found in [4, 9].

## 3.5. Flow Passageways

Flow passageways allow fluid to move from one component to another in a VCS. Pipes are the most common flow passageway, but multi-evaporator systems require additional components, such as flow splits and junctions. Flow passageways can be used to calculate either pressure drops or mass flow rates. It is possible to model a VCS without flow passageways, but their addition in the model can be used to account for various pressure drops and heat transfer that may not be captured without the passageways. Additionally, most VCSs usually incorporate a significant amount of piping in practice since the thermal energy acquisition and rejection are, by design, usually non-collocated. All of the flow passageways are able to handle refrigerant in any one of the three phases: subcooled liquid, superheated vapor, and two-phase mixture.

### 3.5.1. Pipes

Depending on the nature of the upstream and downstream components, it may be necessary to have an intermediate component calculate either mass flow rate or pressure drop. A pipe is capable of either of these calculations. Equations (23), (24), (25), (26), (27) give the pressure loss equations, when mass flow rate is specified. If the mass flow rate is the desired output, the pipe will calculate a mass flow rate, check if the fluid properties associated with this mass flow rate give the correct pressure drop in the pipe, and iterate until a solution is found. The four sources of pressure loss, friction factor,  $\Delta P_f$ , head loss factor,  $\Delta P_K$ , isentropic area,  $\Delta P_J$ , and generic hydraulic resistance,  $\Delta P_R$ , are linearly combined to create the equation for the total pressure loss in the pipe, Equation (27). The four pressure loss terms come from various non-ideal factors in VCS pipes, such as wall roughness, flow direction changes (elbows), physical limits on the amount of fluid flow, etc. Additionally, the pipes allow for heat transfer, as specified in Equation (28)

$$\Delta P_f = \frac{1}{2} \rho u^2 f \frac{L_{eq}}{D_H} \quad (23)$$

$$\Delta P_K = \frac{1}{2} \rho u^2 K_T \quad (24)$$

$$\Delta P_I = \frac{1}{2} \rho \left( \frac{Q}{A_I} \right)^2 \quad (25)$$

$$\Delta P_R = R Q^n \quad (26)$$

$$\Delta P = \Delta P_f + \Delta P_K + \Delta P_I + \Delta P_R \quad (27)$$

$$Q = hA(T_{amb} - T_{pipe}) \quad (28)$$

### 3.5.2. Flow Split and Junction

A split is used when refrigerant flow is channeled from a single stream into multiple streams and a junction is used when multiple streams are collapsed into a single stream. A control volume approach for inlets and outlets is shown in Figure 7. The pressure, Equation (29), and enthalpy, Equation (30), of the liquid in the split/junction are calculated using a control volume approach. The equations are derived from conservation of mass and conservation of energy within the split/junction, respectively. The bulk modulus,  $\beta$ , in (29) captures the refrigerant's resistance to uniform compression. The flow split/junction model requires mass flow rate information for each of the inlets and outlets. Typically this information would come from a valve or compressor, but if a split/junction follows another pressure calculating device, a mass flow rate calculating pipe would need to be used in between these two components.

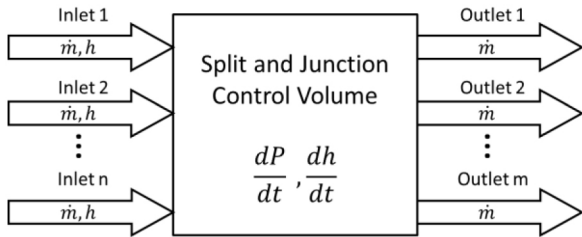


Figure 7. Split and junction control volume for inlets and outlets

$$\frac{dP}{dt} = \frac{\beta}{Vr} \frac{\sum \dot{m}_{in} - \sum \dot{m}_{out}}{\rho} \quad (29)$$

$$\frac{dh}{dt} = \frac{\sum \dot{m}_{in}(h_{in} - h)}{\rho V r} + \frac{1}{\rho} \frac{dP}{dt} \quad (30)$$

Due to the physical size of a typical flow split/junction, the volume term in (29) and (30) can be quite small. This results in very fast dynamics and a computationally stiff problem. A relaxation factor,  $r$ , can be used to artificially slow the dynamics in the split thus improving computational

efficiency. In general, it is important to choose the relaxation factor to balance computational stiffness with computational accuracy for the system. For the validation results given in Section 6, the relaxation factor ranges from 10 to 100,000, depending on the stiffness of the original equation. Despite the addition of the relaxation factor, the time scales of the flow split are still significantly faster than the dynamics of the rest of the system and therefore the relaxation factor does not affect the overall system dynamics for the particular system described below.

## 4. SYSTEM MODELING

Creation of a system model in the Matlab/Simulink environment is straightforward, due to the modularity and ease of use of the components. A multi-evaporator system model is shown in Figure 8. A single buss line is used to transmit information about the thermodynamic state of the fluid between each of the components. Furthermore, when the user opens a component mask, they are able to specify initial operating conditions using intuitive variables, such as pressure and temperature. Flow source and sink blocks, shown in Figure 2, allow for simple generation of a fluid state. A sample use of these blocks is shown in Figure 8. By attaching the source and sink blocks to the secondary fluid ports in the heat exchangers, the user can give constant parameters that determine the ambient conditions for the VCS.

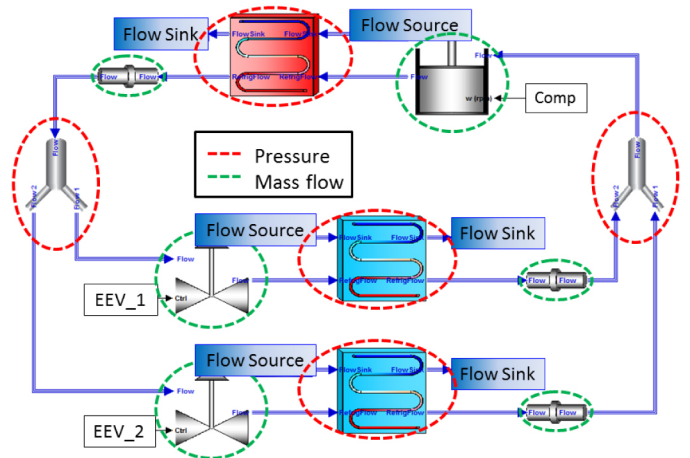


Figure 8. Multi-evaporator system model with pressure and mass flow calculating components highlighted

An additional constraint on VCS modeling arises from calculations of pressure and mass flow rate. Every component in the toolbox calculates one of these two parameters. In order to pass information between components, a mass calculating component must follow downstream of a pressure calculating component and vice versa. In Figure 8, the pressure calculating components are highlighted in red and the mass calculating components are highlighted in green. In order to maintain this pattern, mass calculating pipes were

added into the system downstream of the condenser and downstream of the evaporators.

## 5. EXPERIMENTAL TEST STAND

All of the data collected for validation of the toolbox model was taken from the test stand in [Figure 9](#) at the University of Illinois at Urbana-Champaign [6,15]. The test stand uses R-134a as the refrigerant and was designed to operate in a variety of configurations by including various types of hardware in the VCS through the use of manual valves. This test stand is a dual-evaporator VCS which can be operated as either a single or dual-evaporator system. The manual valves also provide the ability to use four different types of valves: automatic expansion valve (AEV), electronic expansion valve (EEV), orifice tube (OT), and thermostatic expansion valve (TEV). A receiver and accumulator can be introduced to the system using manual valves. The receiver and accumulator insure that subcooled liquid enters the valves and superheated vapor enters the compressor, respectively.



*Figure 9. Image of the University of Illinois test stand*

Additionally, a large number of sensors provide for a variety of measurements during data collection. Mass flow meters directly upstream of the valves measure the refrigerant mass flow rate in each branch of the dual evaporator system. Pressure sensors are present at the inlet and outlet of the evaporators and the inlet and outlet of the compressor. Immersion thermocouples are used to measure the refrigerant temperature at the inlet and outlet of the compressor and condenser and surface thermocouples are used at the inlet and outlet of the evaporators. Finally, thermocouples measure the air temperature at the supply and return of the evaporators and the condenser.

## 6. SYSTEM VALIDATION

Through the use of the native Simulink environment, the ATTMO toolbox is able to simulate VCSs significantly faster than real time. The simulation of a single evaporator VCS for 1000 experimental seconds took approximately 200 seconds using a fixed step solver with a step size of 0.01 seconds, resulting in a 5 time speed up over real time. This speed provides the options of using this model during real time hardware-in-the-loop applications. The simulation time was further reduced to 25 seconds using a variable step, stiff solver, resulting in a 400 time speed up over real time. The simulation was run on a machine with a 3.1 GHz Intel Xeon processor with 6 GB of RAM. This speed is incredibly useful for the design of controllers. From the simple tuning of proportional-integral-derivative (PID) gains to the development of more advanced model predictive controllers, the ability to simulate a system in a matter of seconds instead of hours can significantly reduce controller development time. The ATTMO toolbox can also be used to influence VCS design and component sizing. For example, if the subcooled region at the exit of a condenser is a significant portion of the heat exchanger, the condenser is oversized for the system and reduces system efficiency by having a long subcooled length. The toolbox can be used to easily and quickly determine the appropriate condenser size for realistic static and dynamic operating conditions. The two case studies below show the validation efforts for a single and dual evaporator VCS using the experimental test stand discussed in Section 5. As the ATTMO toolbox was specifically designed with the development of controllers for VCSs in mind, the transient behaviors of these systems is especially important and the simulated system needs to capture these dynamics.

### 6.1. Single Evaporator

For the single evaporator case, the second evaporator on the test stand was removed from the system using the manual valves. The EEV was used to control refrigerant mass flow and the receiver and accumulator were excluded from the system. The model used to simulate this system was similar to the one shown in [Figure 8](#) with the second valve and evaporator removed. The flow junction and flow split blocks remained in the model, but the flow source and flow sink blocks were used to set the mass flow rate through the second flow path to zero. This is achieved by removing the mass calculating components, the pipe and valve, in this branch and forcing a user defined mass flow rate of 0 kg/s in the masks of the flow source and flow sink. In the experiment, a PID controller was used to track a desired refrigerant mass flow rate by adjusting the opening of the EEV. This allowed the user to specify the mass flow rate and the compressor speed independently.

[Figure 10\(a\)](#) shows the inputs used for the single evaporator model validation. The refrigerant mass flow rate was stepped

down at 500 seconds from 0.007 to 0.004 kg/s and then stepped back up at 1000 seconds. The compressor speed was stepped down at 750 seconds from 1800 to 1500 RPM and then stepped back up at 1250 seconds. This set of inputs creates 4 distinct operation conditions. [Figure 10\(b\)](#) shows the measured refrigerant mass flow rate and shows that the PID controller is able to track the desired mass flow rate despite the noise in the measurement. Generally, in addition to the mass flow rate, the two heat exchanger pressures and the superheat of the refrigerant exiting the evaporator are very important to the performance of the system and are typically used to control the cooling capacity of the system. [Figures 10\(c\) - 10\(e\)](#) show the simulation and experimental data for the condenser pressure, evaporator pressure, and the evaporator exit refrigerant superheat.

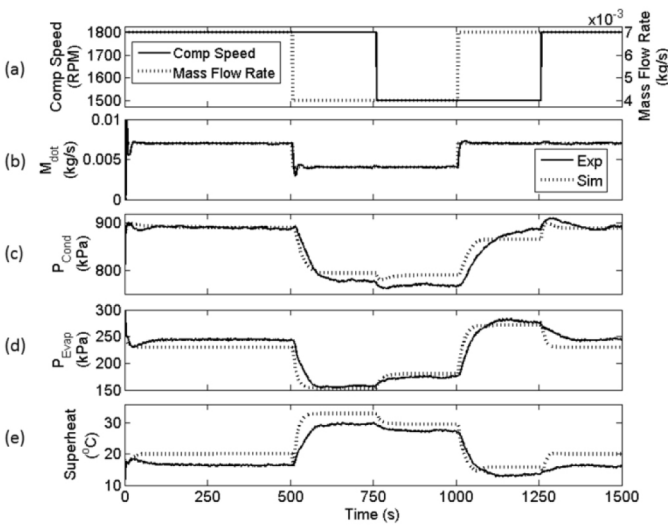


**Figure 10. Single evaporator model (a) input parameters, (b) mass flow rate, (c) condenser pressure, (d) evaporator pressure, (e) evaporator superheat**

In general the simulated dynamics agree very well with the experimental measurements. The simulated heat exchanger pressures deviate from the experimental data by less than 10% except during some of the transitions where the error may be closer to 15%. The evaporator superheat data shows very similar dynamics between the simulation and measured results except for a 3-4°C offset. This offset could easily be due to the fact that a surface thermocouple on the outside of the pipe exiting the evaporator is used to measure the temperature of the refrigerant. By compensating for this constant offset, the error in the simulated superheat is about 5% except during some of the transitions where error approaches 20% for a small period of time. Since the transient dynamics are very important to the development of controllers and steady-state offsets can often be compensated for through feedback control, a fourth-order high-pass Butterworth filter was used with a cutoff of 0.001 Hz. This filter removes any steady-state behavior and isolates the similarities in the transient behaviors. The filter used on both

the experimental and simulation data is shown in [Equation \(31\)](#).

$$G(s) = \frac{0.9918s^4 - 3.967s^3 + 5.951s^2 - 3.967s + 0.9918}{s^4 - 3.984s^3 + 5.951s^2 - 3.951s + 0.9837} \quad (31)$$

The filtered data for the refrigerant mass flow rate, the condenser and evaporator pressures, and the evaporator outlet superheat are presented in [Figure 11\(a\) - \(d\)](#). While there is some deviation between the filtered experimental and simulated results, the dynamics are very similar.

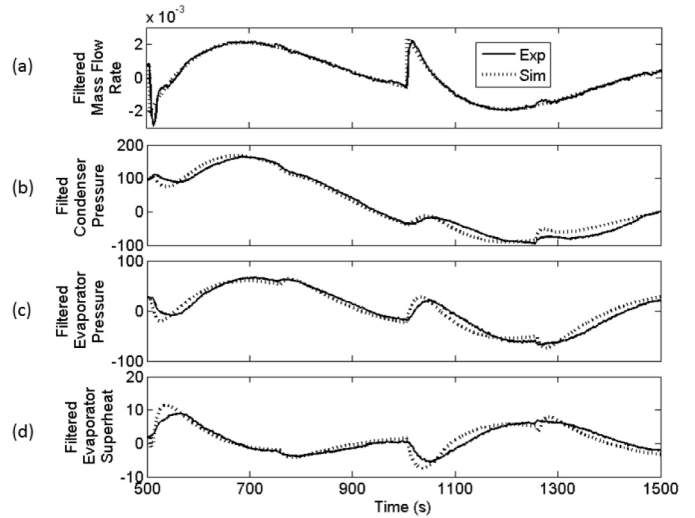


**Figure 11. Filtered single evaporator model (a) filtered mass flow rate, (b) filtered condenser pressure, (c) filtered evaporator pressure, (d) filtered evaporator superheat**

These simulation results show that the ATTMO toolbox is able to accurately model the dynamics of a single evaporator system for several operating conditions both at steady-state and during large transients. This model can be improved by adjusting various parameters as discussed in Section 3 as well as adding pipes and various other components present in the experimental system which are not modeled (e.g. oil separator). The model captures the important dynamics of the system for control purposes and the modeling error is small enough to be compensated for through feedback control.

## 6.2. Dual Evaporator

For the second test case, the second evaporator was introduced into the experimental test stand and was simulated using the model shown in [Figure 8](#). In addition to a more complex system, a more complex set of inputs was used as well. For this case study, the valves were not controlled using a PID controller; valve opening was specified directly. The inputs to the compressor and two EEV are shown in [Figure 12](#). The inputs can be separated in to three regions. Region 1, from 0 - 500 seconds, allows the system to reach a steady-state. Random Gaussian signals were used in Region 2, from

500 - 1500 seconds, to simulate the changes in control inputs that might be seen during a realistic operation of the system. In Region 3, 1500 - 3500 seconds, each control input was stepped up and down independently to determine the effects of each control input on the system dynamics. As previously discussed the transient dynamics are of particular interest. Using the same high-pass filter as the single evaporator case study, [Figures 13, 14, 15](#) show the filtered experimental and simulated dynamics for refrigerant mass flow rates, heat exchanger pressures, and evaporator outlet superheats. Once again, the agreement between the filtered experimental and simulated data is acceptable for control purposes and further model refinement could improve the model accuracy. The largest discrepancies between the two sets of filtered data are clearly in the evaporator outlet superheat temperature, seen in [Figure 15](#). Since the thermocouple used to make this temperature measurement is on the exterior of the pipe at the exit of the evaporator, the thermal conduction through the wall of the pipe could significantly affect the temperature dynamics, causing the observed discrepancies.

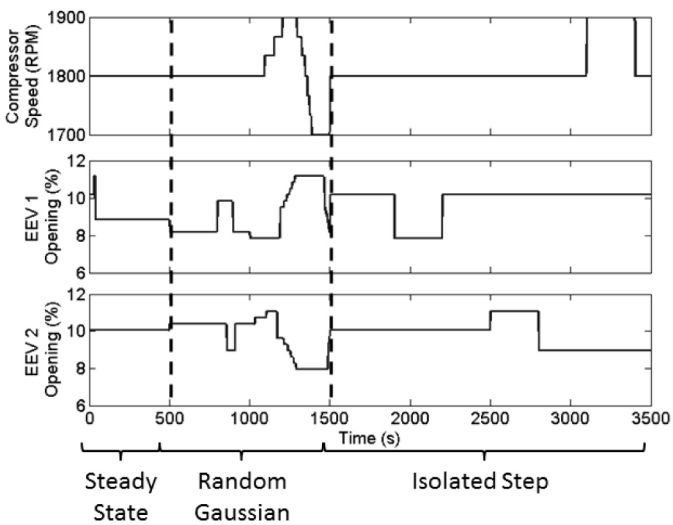


**Figure 12. Inputs to the dual evaporator model**

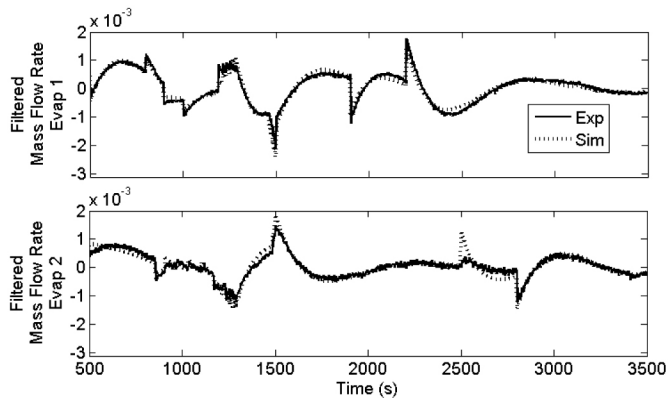


**Figure 13. Filtered dual evaporator model refrigerant mass flow rates**

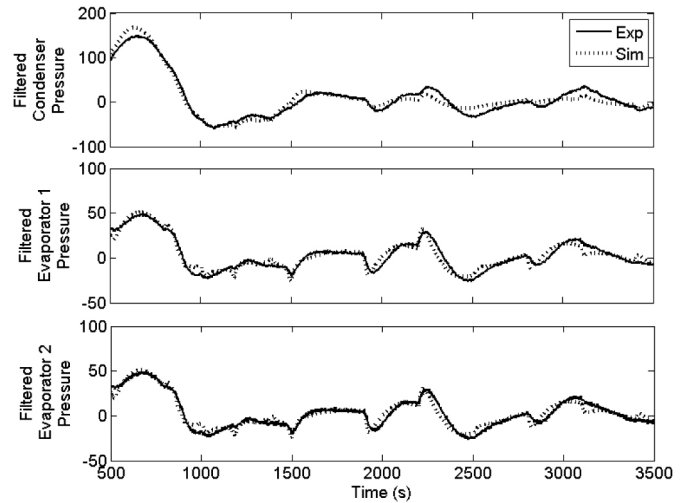


**Figure 14. Filtered dual evaporator model heat exchanger pressures**

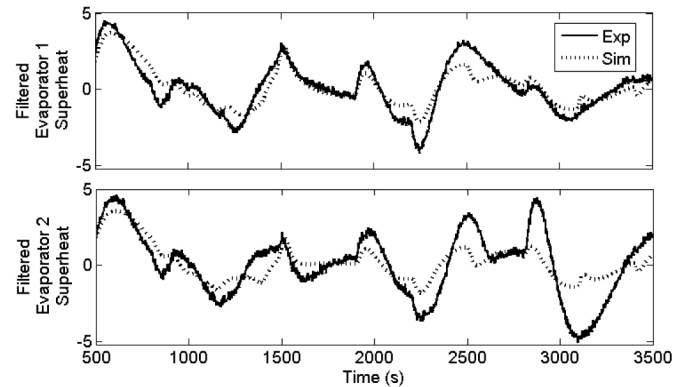


**Figure 15. Filtered dual evaporator model evaporator superheats**

## 7. CONCLUSIONS

The ATTMO toolbox is a user friendly and an accurate modeling tool. The modularity of components allows for a user to “drag and drop” components when constructing a VCS. Additionally, buss lines allow for quick connections between components. As a result, the modeling environment is both flexible and rapidly reconfigurable.

Modeling accuracy is insured by using the Thermosys toolbox as a foundation to the ATTMO toolbox. The single evaporator model output is shown to be in close agreement with the data generated on the experimental test stand, by capturing both transient dynamics and steady-state values. The dual evaporator simulation demonstrates the ATTMO toolbox's ability to predict transient behavior for a more complicated system model with a complex set of system inputs.

All of this is accomplished while permitting the model to run at up to 400 times real time, allowing this tool to be used for

a wide range of applications. Additionally, the simple nature of the user interface allows the component parameters to be quickly tailored to match other experimental VCSs. This means the toolbox can be used to properly size components in a VCS, tune controller gains, and run other computationally intensive exploratory investigations, while requiring minimum modeling time.

## **8. FUTURE WORK**

Although the ATTMO toolbox has demonstrated its efficacy on an existing R-134a system, there is still ample opportunity for expanding its utility. Given the large domain of available heat exchanger configurations, fluids properties, and system designs, it is natural that the future work will focus on building upon the foundation of components described here. Fortunately, the modularity of the toolbox and the buss structures allow for the addition and seamless interfacing of new components. The utility of the toolbox will grow with further usage. As more models of systems are verified and added to the toolbox, the attractiveness to potential users will increase. Current work among the authors is focused on exactly this approach with planned addition of several new models and augmentations of current component models. Moreover, there will be a concerted effort to distribute this tool into other user groups so as to build a community of interest around the toolbox.

## **REFERENCES**

1. McCarthy, K., Walters, E., Heltzel, A., Elangovan, R. et al., "Dynamic Thermal Management System Modeling Electric Aircraft of a More," SAE Technical Paper [2008-01-2886](#), 2008, doi: [10.4271/2008-01-2886](#).
2. Cengel, Yunus A., and Boles, Michael A.. *Thermodynamics: An Engineering Approach*. New York: McGraw-Hill, 2008.
3. Jain, Neera. *Dynamic Modeling and Validation of a Commercial Transport Refrigeration System*. Urbana, Illinois: University of Illinois, MS Thesis, 2009.
4. Li, Bin. *Dynamic Modeling and Control of Vapor Compression Cycle Systems with Shut-down and Start-up Operations*. Urbana, Illinois: University of Illinois, MS Thesis, 2009.
5. Otten, Richard. *Superheat Control for Air Conditioning and Refrigeration Systems: Simulation and Experiments*. Urbana, Illinois: University of Illinois, MS Thesis, 2010.
6. Rasussen, B, and Alleyne, A. "Control-Oriented Modeling of Transcritical Vapor Compression Systems." *Journal of Dynamic Systems, Measurement, and Control*, 2004: 54-64.
7. Li, B, Otten, R, Chandan, V, Mohs, W, Berge, J, and Alleyne, A. "Optimal On-Off Control of Refrigerated Transport Systems." *Control Engineering Practice*, 2010: 1406-1417.
8. Eldredge, Brian. *Improving the Accuracy and Scope of Control-Oriented Vapor Compression Cycle System Models*. Urbana, Illinois: University of Illinois, MS Thesis, 2006.

9. Cheng, T, and Asada, HH. "Nonlinear Observer Design for a Varying-Order Switched System with Application to Heat Exchangers." *Proceedings of the ACC*. Minneapolis, MN, 2006. 2898-2903.

10. He, XD, Liu, S, and Asada, H. "Modeling of Vapor Compression Cycles for Advanced Controls in HVAC Systems." *Proceedings of the ACC*. Seattle, WA, 1995. 3664-3668.

11. Jensen, JM, and Tummeseit, H. "Moving Boundary Models for Dynamic Simulations of Two-Phase Flows." *Proceedings of the Second International Modelica Conference*. Oberpfaffenhofen, Germany, 2002. 235-244.

12. Leducq, D, Guilpart, J, and Trystram, G. "Low Order Dynamic Model as a Vapor Compression Cycle for Process Control Design." *Journal of Food Process*, 2003: 193-199.

13. McKinley, Thomas, and Alleyne, Andrew. "An Advanced Nonlinear Switched Heat Exchanger Model for Vapor Compression Cycles using the Moving-Boundary Method." *International Journal of Refrigeration*, 2008: 1253-1264.

14. Willatzen, M, Pettit, NBOL, and Ploug-Sorensen, L. "A General Dynamic Simulation Model for Evaporators and Condensers in Refrigeration." *International Journal of Refrigeration*, 1998: 398-403.

15. Rasmussen, Bryan. *Dynamic Modeling and Advanced Control of Air Conditioning and Refrigeration Systems*. Urbana, Illinois: University of Illinois, PhD Thesis, 2005.

## **CONTACT INFORMATION**

Andrew Alleyne  
[alleyne@illinois.edu](mailto:alleyne@illinois.edu)  
158 MEB, M/C 244  
1206 W. Green St  
Urbana, IL 61801

## **ACKNOWLEDGMENTS**

This work was supported in part by Air Force Research Laboratory and the National Science Foundation Graduate Research Fellowship.

## **DEFINITIONS/ABBREVIATIONS**

- AEV - Automatic Expansion Valve  
AFRL - Air Force Research Laboratory  
ATTMO - AFRL Transient Thermal Modeling and Optimization  
EEV - Electronic Expansion Valve  
OT - Orifice Tube  
PID - Proportional - Integral - Derivative  
TEV - Thermostatic Expansion Valve

TMS - Thermal Management System

VCS - Vapor Cycle System

## NOMENCLATURE

$A_I$  - Isentropic area [ $m^2$ ]

$A_v$  - Valve area [ $m^2$ ]

$C_d$  - Coefficient of discharge [-]

$cP_{wall}$  - Wall specific heat [ $\frac{kJ}{kgK}$ ]

$D_H$  - Hydraulic diameter [ $m$ ]

$f$  - Friction factor [-]

$G(s)$  - Filter transfer function

$h_f$  - Refrigerant saturated liquid enthalpy [ $\frac{kJ}{kg}$ ]

$h_g$  - Refrigerant saturated vapor enthalpy [ $\frac{kJ}{kg}$ ]

$h_{in}$  - Enthalpy into component [ $\frac{kJ}{kg}$ ]

$h_j$  - Enthalpy in zone [ $\frac{kJ}{kg}$ ]

$h_{out}$  - Enthalpy out of component [ $\frac{kJ}{kg}$ ]

$h_{out,S}$  - Enthalpy out of component, assuming isentropy [ $\frac{kJ}{kg}$ ]

$h_{static}$  - Enthalpy without heat transfer from compressor shell  
[ $\frac{kJ}{kg}$ ] Subscript for zone number

$j$  - In the evaporator, 1=two-phase, 2=superheated In the condenser, 1=superheat, 2=two-phase, 3=subcooled

$K_h$  - User defined constant for compressor enthalpy [-]

$K_m$  - User defined constant for compressor mass flow [-]

$K_T$  - Head loss factor [-]

$K_v$  - User defined constant for valve [-]

$K_y$  - Gain in the mean void fraction [ $\frac{1}{s}$ ]

$L_{eq}$  - Equivalent pipe length [ $m$ ]

$m_{wall}$  - Mass of heat exchanger wall [ $kg$ ]

$\dot{m}_{in}$  - Mass flow rate into component [ $\frac{kg}{s}$ ]

$\dot{m}_{j1j2}$  - Mass flow rate from j1 to j2 [ $\frac{kg}{s}$ ]

$\dot{m}_{out}$  - Mass flow rate out of component [ $\frac{kg}{s}$ ]

$n$  - Hydraulic resistance exponent [-]

$P$  - Pressure [ $kPa$ ]

$Q$  - Volumetric flow rate [ $\frac{m^3}{s}$ ]

$\dot{Q}_j$  - Heat transfer rate in zone j [ $W$ ]

$\dot{Q}_{refj}$  - Refrigerant heat transfer rate in zone j [ $W$ ]

$\dot{Q}_{secj}$  - Secondary fluid heat transfer rate in zone j [ $W$ ]

$R$  - Hydraulic resistance constant [-]

$r$  - Relaxation factor [-]

$t$  - Time [ $s$ ]

$T_r$  - Wall temperature in moving boundary model [ $K$ ]

$T_{wallj}$  - Wall temperature in zone j [ $K$ ]

$u$  - Flow velocity [ $\frac{m}{s}$ ]

$V$  - Volume [ $m^3$ ]

$\beta$  - Bulk modulus [ $kPa$ ]

$\bar{V}$  - Mean void fraction [-] Equilibrium mean void fraction for complete

$\bar{V}_{tot}$  - condensation from saturated vapor to saturated liquid [-]

$\Delta P$  - Pressure difference [ $kPa$ ]

$\Delta P_f$  - Friction factor pressure loss [ $kPa$ ]

$\Delta P_I$  - Isentropic area pressure loss [ $kPa$ ]

$\Delta P_K$  - Head loss factor pressure loss [ $kPa$ ]

$\Delta P_R$  - Generic hydraulic factors pressure loss [ $kPa$ ]

$\zeta_j$  - Fraction of heat exchanger length covered by zone j [-]

$\eta_h$  - Isentropic efficiency for compressor enthalpy [-]

$\eta_m$  - Isentropic efficiency for compressor mass flow [-]

$\rho_j$  - Density [ $\frac{kg}{m^3}$ ]

$\tau_{shell}$  - Compressor shell time constant [ $s$ ]

$\omega$  - Compressor speed [ $rps$ ]

---

The Engineering Meetings Board has approved this paper for publication. It has successfully completed SAE's peer review process under the supervision of the session organizer. This process requires a minimum of three (3) reviews by industry experts.

All rights reserved. No part of this publication may be reproduced, stored in a retrieval system, or transmitted, in any form or by any means, electronic, mechanical, photocopying, recording, or otherwise, without the prior written permission of SAE.

ISSN 0148-7191

Positions and opinions advanced in this paper are those of the author(s) and not necessarily those of SAE. The author is solely responsible for the content of the paper.

**SAE Customer Service:**

Tel: 877-606-7323 (inside USA and Canada)

Tel: 724-776-4970 (outside USA)

Fax: 724-776-0790

Email: [CustomerService@sae.org](mailto:CustomerService@sae.org)

**SAE Web Address:** <http://www.sae.org>

**Printed in USA**

**SAE** *International*<sup>®</sup>